Chapter 4

FRAGMENTATION

In this chapter, we study the kinetics of fragmentation in which an object is continuously broken up into an increasing number of smaller and smaller pieces by an external energy input (Fig. 4.1). Fragmentation is a ubiquitous phenomenon that underlies many natural phenomena and technological processes. At geological time scales, fragmentation is responsible for sand grains on beaches and for mountain boulder fields. At the molecular level, the breaking of individual chemical bonds underlies polymer degradation and the consumption of material in combustion. The most practical example of fragmentation occurs in mineral processing, where the crushing of raw ore is the initial step of mineral extraction. The basic goal in fragmentation is to understand how the distribution of fragment sizes evolves.

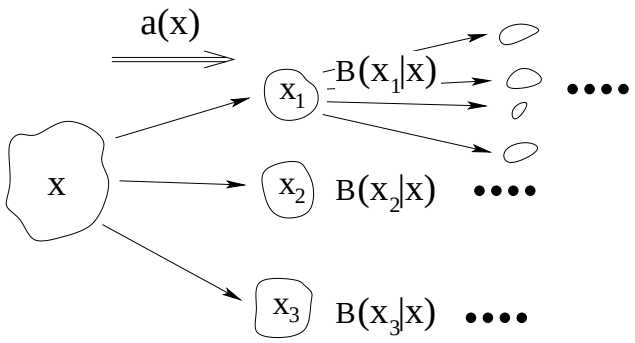

Figure 4.1: Schematic representation of fragmentation. An initial fragment of mass x breaks up at an overall rate $a(x)$ into 3 daughter fragments x_i, $(i = 1, 2, 3)$ with respective production rates $B(x_i|x)$. Each daughter fragment undergoes the same process *ad infinitum*.

As illustrated in Fig. 4.1, a fragmentation event can be visualized as

$$A_x \xrightarrow{a(x)} A_{x_1} + A_{x_2} + \ldots + A_{x_n},$$

in which an object of mass x breaks in a mass-conserving way into n fragments of masses $x_1, x_2, \ldots, x_n$ with $x = x_1 + x_2 + \ldots + x_n$. Here n may be fixed or varying in each breaking event. The overall rate at which an object breaks is specified by $a(x)$, while $B(x_i|x)$ specifies the production rate of a daughter fragment of mass x_i from a fragment of size x. As in aggregation, the fundamental observable is the concentration of fragments of mass x at time t, $c(x,t)$. We want to understand which features of the microscopic interactions, as embodied by the break-up rates $a(x)$ and $B(x_i|x)$, determine this distribution. In the spirit of our treatment of aggregation from the previous chapter, we will outline basic features that emerge from the solutions of the master equations for illustrative case studies. We will then apply scaling to determine solutions to the master equations. As in the case of aggregation, the scaling approach is a simple, yet powerful method that gives a universal classification for the solutions to the master equation.

The Master Equation

the master equation that describes the evolution of the mass distribution is:

$$\frac{\partial c(x,t)}{\partial t} = -a(x)\, c(x,t) + \int_x^\infty c(y,t)\, a(y)\, B(x|y)\, dy. \tag{4.1}$$

The first term on the right-hand side accounts for the loss of fragments of mass x due to their breakup at overall rate $a(x)$. The second term accounts for the gain of fragments of size x from the breakup of objects mass larger than x. The master equation again represents a mean-field description, and it is useful to highlight the underlying approximations in this approach in the context of fragmentation. They include:

- Shape independence. The role of fragment shape on the evolution is not considered.
- Spatial homogeneity. The fragment densities are independent of spatial position.
- Linearity. The breakup properties of a given cluster does not depend on the state of any other clusters.

4.1 Binary Breakup

Binary breakup represents a simple special case in which two fragments are created in each breaking event. The master equations may also be written in a form that explicitly highlights the binary nature of the breaking:

$$\frac{\partial c(x,t)}{\partial t} = -c(x,t) \int_0^x F(y, x-y)\, dy + 2 \int_x^\infty c(y,t)\, F(x, y-x)\, dy. \tag{4.2}$$

Here $F(u,v)$ is the overall rate at which a fragment of mass $u+v$ breaks up into fragments of masses u and v. The factor 2 in the last term accounts for the fact that either one of the daughter fragments from the breakup of a cluster of size y may be of size x. By comparing with Eq. (4.1), we have $a(x) = \int_0^x F(y, x-y)\, dy$. Symmetry in the interchange of the two daughter fragments also implies that $B(x|y) = B(y-x|y)$. In the natural situation where the overall breakup rate does not depend on the masses of the two output fragments, $F(y, x-y) \equiv f(x)$ is independent of y. Then the coefficient multiplying $c(x,t)$ on the right side of Eq. (4.3) becomes $xf(x)$; we identify this factor as the overall breakup rate $a(x)$ from (4.1). Now the master equation can be written as

$$\frac{\partial c(x,t)}{\partial t} = -xf(x)c(x,t) + 2 \int_x^\infty c(y,t)\, f(y)\, dy. \tag{4.3}$$

Perhaps the simplest example of binary breakup is *random scission*, where the breakup rate equals the fragment size, $a(x) = x$. Such a choice naturally describes in the breaking of a linear polymer by chemical attack where each bond is broken at a fixed rate. If we visualize the unbroken polymer as line segments (Fig. 4.2), random scission is equivalent to the random cutting of this line, with cuts occurring at a fixed rate per unit length. For random scission, the master equations are

$$\frac{\partial c(x,t)}{\partial t} = -xc(x,t) + 2 \int_x^\infty c(y,t) dy, \tag{4.4}$$

where we assume a scission rate of 1 per unit length.

We first exploit the cutting picture to construct a purely probabilistic solution for the fragment size distribution starting with an initial fragment of length L. Since the number of cuts is proportional to the time t, any segment of length Δx will be cut with probability $t\Delta x$, while the probability that the segment has not been cut by time t equals $e^{-t\Delta x}$. Since each fragment is part of the initial line segment, there are 3 possibilities: (i) the initial segment could remain intact, (ii) a fragment is at one end of the segment, (iii) a fragment is in the interior. We evaluate the respective probabilities for these cases.

0 Intact segment. Since the average number of cuts is Lt, the segment remains intact with probability e^{-Lt}. The length distribution for zero cuts is $p_0(x) = e^{-Lt}\delta(x-L)$.

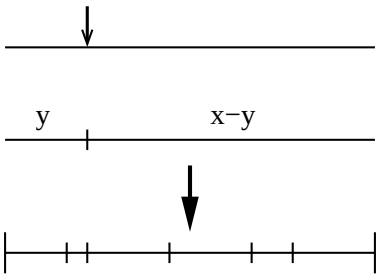

Figure 4.2: Random scission. An initial segment of length x is cut at a random point into two segments of lengths y and $x-y$. A sequence of such events can be viewed as the random deposition of cuts (bottom).

1 End fragment. An end fragment of length in the range $(x, x+dx)$ is created when there are no cuts within a distance x from the end (probability e^{-xt}), and the interval $(x, x+dx)$ contains a cut (probability $t\,dx$). The probability for this event is $p_1(x)dx = 2t\,e^{-xt}\,dx$, where the factor 2 accounts for both endpoints. Therefore the length distribution for such segments is $p_1(x) = 2te^{-xt}$.

2 Interior fragment. Such a fragment arises when there are two cuts in the intervals dx and dz at opposite ends of a otherwise intact fragment of length x. The probability for this event is $t^2e^{-xt}dx\,dz$. Integrating over all possible fragment positions $(x < z < L)$ gives $p_2(x) = t^2(L-x)e^{-xt}$.

Combining the three events gives the probability for a fragment of length x at time t:

$$c(x,t) = e^{-xt}\left\{\delta(L-x) + \left[2t + t^2(L-x)\right]\Theta(L-x)\right\}. \tag{4.5}$$

It is easy to check that this expression is a solution of the master equation (4.4).

Because of the linearity of the master equations, the distribution for an arbitrary initial distribution $c(x, t=0) \equiv c_0(L)$ is obtained by averaging Eq. (4.5) over this distribution. Thus

$$c(x,t) = e^{-xt}\left\{c_0(x) + \int_x^\infty c_0(y)\left[2t + t^2(y-x)\right]dy\right\}. \tag{4.6}$$

The dominant feature of this exact solution is the overall exponential decay so that fragments rapidly shrink. Since the number of segments grows linearly with time, segments in the interior become dominant and the influence of the initial segment boundaries disappears. From Eq. (4.6), the asymptotic size distribution is

$$c(x,t) \simeq L_0 t^2\, e^{-xt} \tag{4.7}$$

with $L_0 = \int x c_0(x)\,dx$ the average initial fragment size. This asymptotic form can be written in the scaling form $c(x,t) \simeq L_0 s^{-2}\,\Phi(xs^{-1})$, with typical size $s(t) = t^{-1}$ and $\Phi(x) = \exp(-x)$. The exponential initial condition, $c_0(x) = \exp(-x)$, the fragment size distribution is particularly simple, $c(x,t) = (t+1)^2 e^{-x(t+1)}$.

An alternative, and extremely useful approach is known as the *Charlesby Method*. This approach is essentially nothing more than a Taylor expansion of the fragment size distribution in time. A key feature of the method is that the expansion coefficients can be solved recursively so that the full series can be obtained. Thus even though the Taylor expansion ostensibly is suitable for short times, the ability to determine all the terms in this expansion makes this method exact. The random scission model provides a nice illustration of the method.

It is first convenient to write $c(x,t)$ as $e^{-xt}F(x,t)$. This construction leads to a master equation for F that has only a gain term. We then write the $F(x,t)$ as the power series so that

$$c(x,t) = e^{-xt}\sum_{k=0}^{\infty} t^k f_k(x). \tag{4.8}$$

The lowest-order term is dictated by the initial condition, $f_0(x) = c_0(x)$. Substituting this expansion into the rate equation (4.4), and differentiating once with respect to x, yields the recursion relation for the expansion functions

$$\frac{d}{dx} f_k(x) = \frac{3-k}{k+1} f_{k-1}(x). \tag{4.9}$$

The first two functions obey $\frac{d}{dx} f_1(x) = 2f_0(x)$ and $\frac{d}{dx} f_2(x) = \frac{1}{2} f_1(x)$. Integrating these equations successively yields

$$f_1(x) = 2\int_x^\infty P_0(x)dx, \qquad f_2(x) = \int_x^\infty (y-x)P_0(y)dy. \tag{4.10}$$

The $k = 3$ term vanishes and so do all subsequent terms: $f_k = 0$ for all $k \geq 3$. The resulting solution then coincides with (4.6). The Charlesby method is straightforward to implement, but it can be quite powerful.

Finally, we present a direct solution to the master equation (4.4). By moving the first term on the right side of Eq. (4.4) to the left, the master equation has the form $\frac{\partial(cI)}{\partial t} = J(t)$, where the integrating factor $I = e^{x(t+B_0)}$, with B_0 a constant and J is the last term on the right side of (4.4) multiplied by the integrating factor. This observation suggests that we seek a solution of the form $c(x,t) = A(t)\, e^{-x(t+B_0)}$. Now it is convenient to differentiate the master equation with respect to x to convert it to the partial differential equation $c_{xt} = -xc_x - 3c$, where the subscripts denote partial differentiation. Substituting the ansatz $c = A\, e^{-Bx}$ into this equation and then equating separately the resulting terms that are independent and linear in x gives $\dot{A} = 2A/B$ and $\dot{B} = 1$. The solution then is

$$c(x,t) = A_0(t+B_0)^2\, e^{-(t+B_0)x}. \tag{4.11}$$

discussion incomplete.

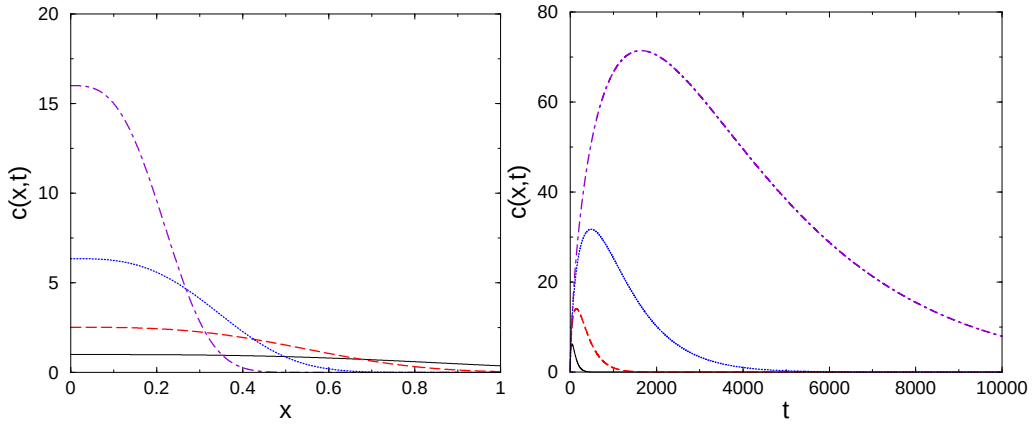

Figure 4.3: (Left) The asymptotic fragment size distribution (4.14) for the case $\lambda = 3$ as a function of x for $t = 1$ (solid) ,4 (dash) ,16 (dotted), and 64 (dot-dash). (Right) The same fragment size distribution as a function of t for $x = \frac{1}{4}$ (solid), $\frac{1}{6}$ (dash), $\frac{1}{9}$ (dotted), and $\frac{1}{13.5}$ (dot-dash).

By the direct approach, we can also treat the problem of homogeneous scission in which the overall breakup rate of a cluster is $a(x) \sim x^\lambda$, for general λ. The master equation is now

$$\frac{\partial c(x,t)}{\partial t} = -x^\lambda\, c(x,t) + 2\int_x^\infty y^{\lambda-1} c(y,t)\, dy. \tag{4.12}$$

Following the same approach as in random scission, we seek a solution of the form $c(x,t) = A(t)e^{-x^\lambda(t+B_0)}$. Substituting this into the master equation yields a soluble ordinary differential equation for $A(t)$, from which one obtains a special solution for $c(x,t)$,

$$c(x,t) = (1 + t/B_0)^{2/\lambda} e^{-(t+B_0)x^\lambda}. \tag{4.13}$$

By the linearity of the master equations, the general solution for $c(x,t)$ can be written as a linear combination, that is, an integral transform of Eq. (4.13), which, in turn, can be expressed in terms of special functions. In the long-time limit, the asymptotic behavior is

$$c(x,t) \propto t^{2/\lambda} \exp(-tx^{\lambda}). \tag{4.14}$$

A sketch of this fragment size distribution is shown in Fig. 4.3, both as a function of time for fixed size, and as a function of size at fixed times. Qualitatively, the behavior is in accord with simple-minded intuition. The population of a given (small) size, x, initially grows due to the breakup of larger fragments. Eventually, however, this size population decays when the production of x diminishes due to the depletion of larger fragments. This decay is asymptotically exponential, with the decay time varying inversely in the particle size. For the distribution at fixed time, there is a steepening near the origin as a function of time, reflecting the eventual predominance by very small fragments. This small mass tail often has a power law form, as discussed previously. Notice also that this asymptotic form for $c(x,t)$ becomes pathological as $\lambda \to 0$. This is a signal of the shattering transition, which will be discussed in a later section.

A particularly interesting special case is when the homogeneity exponent equals zero. For $F(x,y) \propto (x+y)^{-1}$, the exact solution for the fragment size distribution in the limit $\lambda \to 0$ is,

$$c(x,t) = e^{-t}\delta(x-l) + \frac{2te^{-t}}{l} \sum_{n=0}^{\infty} \frac{[2t\ln(l/x)]^n}{n!\,(n+1)!}. \tag{4.15}$$

In the small mass limit, a singularity in $c(x,t)$ develops due to the explosive growth in the number of very small fragments. The corresponding moments of this fragment size distribution are,

$$M_n(t) = l^n \exp[(1-n)t/(1+n)]. \tag{4.16}$$

Thus the total number of fragments, $M_0(t)$, grows exponentially in time, in contrast to the power law growth for $M_0(t)$ in the non-shattering regime. As we shall see, this solution corresponds to a system on the borderline between scaling and shattering.

4.2 Scaling

We now present a scaling approach to determine the asymptotic behavior of the fragment size distribution. As in aggregation, the applicability of scaling rests on the hypothesis that a well-defined typical size scale arises that decreases to zero with time. Consequently, the fragment size distribution should be a function *only* of the ratio of the size of a fragment to this typical size. Using this scaling ansatz, we can determine the asymptotic form of the fragment size distribution quite simply for general breakup rates. As in aggregation, we assume that the breakup rates are homogeneous functions. The overall breakup rate depends on the fragment mass as $a(x) = x^{\lambda}$, thereby defining the homogeneity index λ. Physically, we might expect a larger fragment to be more fragile so that λ should be positive. Homogeneity also implies that the daughter fragment distribution $B(x|y)$ depends only on the ratio of the daughter fragment mass to that of the initial fragment, $B(x|y) \propto y^{-1}\, b(\frac{x}{y})$. By definition, the integral $\int_0^{\infty} b(x)\,dx$ equals the average number of fragments produced in a single breakup event, and mass conservation imposes the condition $y = \int_0^y x\, B(x|y)\,dy$; in scaled form, this statement becomes $\int_0^1 x\, b(x)\,dx = 1$.

Let's start by investigating the moments of the fragment size distribution. Define $M_\alpha(t)$ as the α^{th} moment of this distribution, $M_\alpha(t) = \int_0^{\infty} x^\alpha\, c(x,t)\,dx$. We determine the time dependence of M_α by multiplying the master equation (4.1) by x^α and integrating over all x to give

$$\int_0^{\infty} x^\alpha \left[\frac{\partial c(x,t)}{\partial t} = x^{\lambda+\alpha} c(x,t) + x^\alpha \int_x^{\infty} c(y,t) y^{\lambda-1} b(x/y)\,dy \right]. \tag{4.17}$$

We make use of a simple trick, that will be used repeatedly, to yield a closed equation for the moments (see

Fig. 4.4). For the second term on the right side, we interchange the order of the integrations to give

$$\begin{aligned}\int_0^\infty x^\alpha \int_x^\infty c(y) y^{\lambda-1} b(x/y)\, dy &= \int_0^\infty y^{\lambda-1} c(y)\, dy \int_0^y x^\alpha b(x/y) dx \\ &= \int_0^\infty y^{\lambda+\alpha} c(y)\, dy \int_0^1 z^\alpha b(z)\, dz \qquad z = x/y \\ &= M_{\alpha+\lambda} L_\alpha,\end{aligned}$$

where $L_\alpha = \int_0^1 x^\alpha b(x)\, dx$ is the $\alpha^{\rm th}$ moment of the scaled daughter breakup kernel.

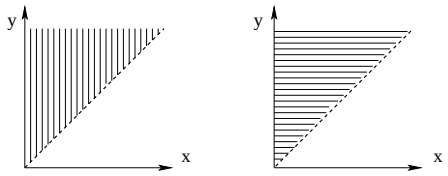

Figure 4.4: Interchanging the integration order in Eq. (4.23). Left: illustration of integrating over y from x to ∞ and then over all x. Right: integrating over x for 0 to y and then over all y.

Thus the moments obey the rate equation

$$\dot{M}_\alpha = (L_\alpha - 1)\, M_{\alpha+\lambda}. \tag{4.18}$$

Starting with $M_1(t) = 1$, Eq. (4.18) gives $\dot{M}_{1-\lambda}(t) = (L_{1-\lambda} - 1)$, so that $M_{1-\lambda}(t) = (L_{1-\lambda} - 1)t + \text{const.}$. Here $L_{1-\lambda} - 1$ is a positive constant for $\lambda < 1$. Iterating leads to the asymptotic solution,

$$M_{1-k\lambda} \simeq \prod_{j=1}^{k} (L_{1-j\lambda} - 1)\, \frac{t^k}{k!} \;\propto\; t^k, \tag{4.19}$$

for the discrete set of equidistant index values $1 - k\lambda$. Thus the negative moments, $M_{1-k\lambda}$, with k a positive integer, are connected recursively, and asymptotically grow as t^k. These negative moments play a role analogous to that of the positive integer moments of the cluster size distribution in aggregation.

Let's now apply scaling to determine the asymptotics of the fragment size distribution itself. Just as in aggregation (see Eq. (3.40)), the scaling ansatz for the size distribution in fragmentation is

$$c(x,t) = \frac{1}{s^2}\, f\Big(\frac{x}{s}\Big), \tag{4.20}$$

where $s(t)$ is the typical fragment mass, and the exponent -2 enforces mass conservation. We now substitute the scaling ansatz (4.20) into the master equation, Eq. (4.1). This step separates the time dependence and the dependence of the scaled fragment size distribution on scaled mass $u \equiv x/s$:

$$\begin{aligned}\dot{s}\, s^{-(1+\lambda)} &= -\omega \\ \omega[2f(u) + u\, f'(u)] &= -u^\lambda\, f(u) + \int_u^\infty f(v)\, v^{\lambda-1}\, b\Big(\frac{u}{v}\Big)\, dv,\end{aligned} \tag{4.21}$$

where $\omega > 0$ is the separation constant.

From the first equation, the typical fragment mass has the asymptotic time dependence,

$$s(t) \sim \begin{cases} t^{-1/\lambda}, & \text{for } \lambda > 0, \\ e^{-\omega t}, & \text{for } \lambda = 0, \\ (t_c - t)^{1/|\lambda|}, & \text{for } \lambda < 0 \text{ and } t \to t_c, \end{cases} \tag{4.22}$$

where $t_c = (s(0)\lambda\omega)^{-1}$. Here again is a demonstration of the utility of the scaling approach: with essentially no labor, we've determined the time dependence of the average fragment mass! For positive λ, the typical

mass decreases as a power law in time. However, as λ becomes smaller, the breakup of small fragments becomes relatively more important. When λ becomes less than zero, the fragmentation of the tiniest fragments occurs so quickly that the mean fragment mass vanishes at a finite time t_c. This singularity is the *shattering* transition and is the analog of gelation in an aggregating system with a homogeneity index larger than one. For $t > t_c$, a finite fraction of the mass is converted into a dust phase that contains a finite fraction of the total mass, but consists of an infinite number of zero mass particles.

Let's begin by studying the equation for scaled form of the fragment mass distribution. Here we exploit the linearity of the master equation to compute an infinite set of moments of the fragment size distribution. With these moments, we can then reconstruct the fragment size distribution itself. In the scaling regime $\lambda > 0$, we convert this equation into a relation for the moments of $f(u)$, by multiplying both sides of Eq. (4.21) by u^α and integrating over all u. Here we define the $\alpha^{\rm th}$ moment of the scaling function by $m_\alpha = \int_0^\infty x^\alpha\, f(x)\, dx$. After integrating by parts, the left-hand side is simply $\omega(1-\alpha)m_\alpha$. For the right-hand side, we interchange the order of integration to transform (see again Fig. 4.4)

$$\int_0^\infty u^\alpha \int_u^\infty v^{\lambda-1}\, f(v)\, b(u/v)\, dv \qquad \text{to} \qquad \int_0^\infty v^{\lambda-1}\, f(v)\, dv \int_0^v u^\alpha\, b(u/v)\, du. \tag{4.23}$$

We then express the second integral in the scaled variable $w = u/v$ and define the moments of the scaled daughter breakup kernel $L_\alpha \equiv \int_0^1 x^\alpha\, b(x)\, dx$ to obtain the linear recursion relation for the moments of the scaling function, in close analogy with Eq. (4.18),

$$m_{\alpha+\lambda} = \omega\, \frac{1-\alpha}{L_\alpha - 1}\, m_\alpha. \tag{4.24}$$

The explicit dependence on the kernel is contained *only* in L_α. Thus the fragment size distribution will depend only on the homogeneity index of the overall breakup rate and on the limiting behavior of L_α. Notice that for a system that obeys scaling, *e.g.*, Eq. (4.20), the "bare" and the "scaled" moments are related by $M_\alpha(t) = m_\alpha \times s(t)^{\alpha-1}$. The special case $\alpha = 0$ yields $s(t) = m_0/M_0(t)$; thus the average size is inversely proportional to the average number of fragments.

An important technical point is that m_α is essentially the *Mellin transform* of the fragment size distribution. If the Mellin transform of a function is known, we can then use well-established rules for inverting Mellin transforms to reconstruct the function itself. For the problem of fragmentation, we have found the moments for an infinite discrete set of α values. Thus we also need to invoke the natural hypothesis that these moments vary smoothly in the intervening range between this set of *alpha* values.

The Mellin Transform

The Mellin transform of a function $c(x)$ is defined by

$$M(s) = \int_0^\infty c(x)\, x^{s-1}\, dx.$$

The Mellin transform is just the moment of order $s-1$ of the function $c(x)$. Notice also that the Mellin transform is just a Laplace transform in disguise. Thus we can adapt the better-known rules about inverting the Laplace transform to infer the inverse of Mellin transforms. Here are two basic rules about the Mellin transform: (i) if $M(s)$ is the Mellin transform of $c(x)$, then $M(s-n)$ is the Mellin transform of $x^{-n}c(x)$, (ii) the Mellin transform of $x^{-m}\int_x c(y)y^{m-1}dy$ is $(s-m)^{-1}M(s)$.

The large-mass tail of the fragment mass distribution (scaled mass $x \to 1$) can be probed by studying the high-order moments, m_α for large α. Here the relevant quantities are not the positive integer moments, but the moments of order $\alpha = k\lambda$, with k a positive integer. For such values, we iterate Eq. (4.24) and use $m_0 = 1$. This yields

$$m_{k\lambda} = \omega^{k-1} \prod_{n=1}^{k-1} \frac{n\lambda - 1}{1 - L_{n\lambda}}. \tag{4.25}$$

For large k, the product is dominated by the factors with large n. In this limit, the form of $L_{n\lambda}$ is determined by the behavior of the breakup kernel $b(x)$ for $x \to 1$. This is limit where a fragment remains nearly intact in

breaking event, except for the creation of an infinitesimal dust particle. For this limit, a generic form of the kernel is $b(x) = b(1) + \mathcal{O}((1-x)^\mu)$, for $x \to 1$, where $b(1) \geq 0$, the probability for no breaking to occur, and $\mu > 0$ are constants. Then $L_\alpha = b(1)/\alpha + \mathcal{O}(\alpha^{-(\mu+1)}) \sim b(1)/\alpha$ for large α. Using this form in Eq. (4.25), we find after several straightforward steps,

$$m_\alpha \propto \left(\frac{\omega\alpha}{e}\right)^{\alpha/\lambda}\ \alpha^{(b(1)-1)/\lambda - 1/2}, \qquad \text{for } \alpha \to \infty. \tag{4.26}$$

The non-trivial dependence on the breakup kernel appears only through λ in the controlling factor, $\alpha^{\alpha/\lambda}$, and through $b(1)$ and λ in the correction term, $\alpha^{(b(1)-1)/\lambda}$. This universality of m_α leads, through the inverse Mellin transform, to the following universal expression for the fragment size distribution

$$f(x) \sim x^{b(1)-2}\ \exp(-a\,x^\lambda) \qquad x \to \infty, \tag{4.27}$$

where $a = 1/(\lambda\omega)$. By comparing with the scaling ansatz, the large mass tail of the distribution is gives

$$c(x,t) \propto \exp(-\text{const.} \times t\,x^\lambda). \tag{4.28}$$

This asymptotic behavior matches that from exact results of homogeneous binary fragmentation models.

In the small-mass limit, we need the moments of large negative order. Accordingly, we choose $\alpha = 1 - k\lambda$ in Eq. (4.24) and iterate to arrive at the counterpart of Eq. (4.25),

$$m_{1-k\lambda} = \omega^{-k}\,\frac{\prod_{n=1}^{k}[L_{1-n\lambda} - 1]}{\prod_{n=1}^{k} n\lambda}. \tag{4.29}$$

Here the k dependence of $m_{1-k\lambda}$ for large k is now determined by the limiting form of $b(x)$ for x near 0. There are two generic cases for this limiting form. One is the situation of break-up kernels $b(x)$ with a strict cutoff at small size, *i.e.*, no clusters below a fixed relative size $x_0 < 1$ are produced in a single breakup event. From the definition of L_α, the moment $L_{1-\alpha}$ has the leading behavior $x_0^{-\alpha}/\alpha^{1+\mu}$ for large α. Substituting this form into Eq. (4.29) yields

$$m_{1-k\lambda} \sim \frac{1}{k!}\frac{1}{(\omega\lambda)^k}\,x_0^{\lambda+2\lambda+\cdots+k\lambda}\ \propto\ x_0^{-k^2\lambda/2}. \tag{4.30}$$

Thus the controlling factor of $m_{-\alpha}$ in the large α limit is

$$m_{-\alpha} \sim \exp\left[\frac{-\ln x_0}{2\lambda}\,\alpha^2\right] \qquad \alpha \to \infty, \tag{4.31}$$

whose inverse Mellin transform yields the classical log-normal form for the controlling factor of $f(x)$,

$$f(x) \sim \exp\left[-\frac{\lambda}{2\ln x_0}(\ln^2 x)\right] \qquad (x \to 0). \tag{4.32}$$

The log-normal form is expected naively as the mass of a given fragment schematically evolves as $x_0 \to x_1 \to x_2 \to \cdots \to x_N$, where the successive reduction factor, $r_k = x_k/x_{k-1}$, is a random variable with a well-behaved distribution. By the central limit theorem, $\log x_N = \sum_{k=0}^{N} \log r_k$ will be normally distributed, so that x_N will be distributed log-normally.

A second general class of fragment mass distributions arises for kernels in which single fragmentation event gives rise to a non-vanishing production of arbitrarily small clusters. The absence of a cutoff in the breakup kernel is typified by the power law form $b(x) \sim x^\nu$ for small x. Thus from Eq. (4.24), m_α diverges whenever L_α diverges. This divergence occurs for α less than a critical value α_c, which is less than 0, since m_0 is finite. For α close to α_c we keep only the leading term in Eq. (4.24) to give

$$m_\alpha \simeq L_\alpha\,\frac{m_{\alpha_c+\lambda}}{\omega\,(1-\alpha_c)} \propto L_\alpha. \tag{4.33}$$

Since m_α is proportional to L_α, it follows that $f(x)$ coincides with $b(x)$. That is $f(x)$ has the power law form

$$f(x) \sim x^\nu, \qquad \text{as } x \to 0. \tag{4.34}$$

Thus for a breakup kernel with no small size cutoff, the limiting form of $f(x)$ now decays as x^ν compared to the more rapidly varying log-normal bound, $\exp[-c\,(\ln x)^2]$ for a kernel with a small size cutoff.

4.3 Fragmentation with Input

Fragmentation with a steady input of material arises in many materials production processes, such as the crushing of mineral ore, where the input is the raw ore. Let the input rate of objects of size x be $I(x)$, with the total mass input rate set to unity, $\int xI(x)dx = 1$. Because of the linearity of the master equations, we can treat the case of a general input with no additional complications beyond to the case of monodisperse input. Let's analyze the effect of a general input for the simplest case of random scission with overall breakup rate $a(x) = x$. The master equation is

$$\frac{\partial c(x,t)}{\partial t} = -xc(x,t) + 2\int_x^\infty c(y,t)dy + I(x). \tag{4.35}$$

Then using the same interchange of the order of integrate that was illustrated in Eq. (4.23), the Mellin transform $c(s,t) = \int c(x,t)\, x^{s-1}dx$ evolves according to

$$\frac{\partial c(s,t)}{\partial t} = \left(\frac{2-s}{s}\right) c(s+1,t) + I(s), \tag{4.36}$$

where $I(s) = \int I(x)x^{s-1}dx$, is the Mellin transform of the input rate.

In the steady state, the Mellin transform satisfies $c(s+1) = (\frac{s}{s-2})I(s)$ or, after shifting the index s by 1

$$c(s) = \left(\frac{s-1}{s-3}\right) I(s-1). \tag{4.37}$$

Using basic facts about the properties of the Mellin transform that we outlines in the last section, the steady-state fragment size distribution is

$$c(x) = x^{-1}I(x) + 2x^{-3}\int_x^\infty I(y)y\, dy. \tag{4.38}$$

The second term is dominant in the limit of small fragment sizes. Since the integral approaches 1 as $x \to 0$, the size distribution has the universal algebraic tail

$$P(x) \simeq 2x^{-3}. \tag{4.39}$$

For any well-behaved input, this size distribution is independent of the details of the input.

This asymptotic distribution can also be obtained by the following heuristic reasoning. Because of the steady input, the total mass in the system, $M(t) = c(s=2,t)$, grows linearly with time, $M(t) = t$. Similarly, from the master equation (4.35), the total number of fragments $N(t) = c(s=1,t)$ satisfies $\frac{d}{dt}N(t) = t + \mu$, where $\mu = \int I(x)dx$ is the number of fragments added per unit time. Consequently, $N(t) = \frac{1}{2}t^2 + \mu t$. The first two moments imply that the typical fragment size is $M/N \sim t^{-1}$. Thus the fragment mass distribution is expected to approach the scaling form in the long-time limit

$$P(x,t) \simeq t^3 F(xt), \tag{4.40}$$

with a prefactor t^{-3} to ensure that the total mass in the system grows linearly with time. With this scaling form, a steady state is possible only when $F(z) \sim z^{-3}$ for small x. This fact implies that $P(x) \sim x^{-3}$.

The full time-dependent solution can be obtained by the Charlesby method and thus we can establish the scaling behavior rigorously. To this end, we expand the Mellin transform as a power series in time

$$c(s,t) = \sum_{n=1}^\infty \frac{t^n}{n!}\, c_n(s) \tag{4.41}$$

and then solve the expansion functions $c_n(s)$ iteratively. A constant term is absent in this expansion if we take the system to be initially empty. Performing the Mellin transform of the master equation (4.35), substituting in this expansion, and equating similar powers of time yields $c_1(s) = I(s)$ and $c_{n+1}(s) = -\frac{s-2}{s}c_n(s+1)$ for $n \geq 2$. Solving this set of equations recursively gives

$$c_{n+1}(s) = (-1)^n \frac{(s-1)(s-2)}{(s+n-1)(s+n-2)} I(s+n).$$

To invert this Mellin transform, we re-write $c_{n+1}(s)$ as the partial fraction expansion

$$c_{n+1}(s) = (-1)^n \left[1 - \frac{n(n+1)}{s+n-1} + \frac{n(n-1)}{s+n-2}\right] I(s+n).$$

From Eq. (4.41), the fragment size distribution can be written as a power series

$$c(x,t) = \sum_{n=0}^{\infty} \frac{t^{n+1}(-x)^n}{(n+1)!} c_n(x), \tag{4.42}$$

where the inverse transform of $c_{n+1}(s)$ has been conveniently written as $(-x)^n c_n(x)$. The three terms in the above expression for $c_{n+1}(s)$ can be inverted using the rules outlined before Eq. (4.38). The final expression for $c_n(x)$ reads

$$c_n(x) = I_1(x) + \frac{n(n+1)}{x} I_2(x) + \frac{n(n-1)}{x^2} I_3(x), \tag{4.43}$$

with

$$I_1(x) = I(x) \quad I_2(x) = \int_x^\infty I(y)\, dy \quad I_3(x) = \int_x^\infty y f(y)\, dy. \tag{4.44}$$

Summing the three terms separately gives the fragment size distribution

$$c(x,t) = \sum_{k=1}^{3} t^k I_k(x) F_k(xt), \tag{4.45}$$

with the scaling functions

$$\begin{aligned} F_1(z) &= z^{-1}(1 - e^{-z}), \\ F_2(z) &= e^{-z}, \\ F_3(z) &= z^{-3}\left[2 - (2 + 2z + z^2)e^{-z}\right]. \end{aligned} \tag{4.46}$$

The function $F_3(z)$ has been obtained from the power series $F_3(z) = \sum_{n\geq 0} \frac{(-z)^n}{n!(n+3)}$. One can verify that the previous results for $N(t)$, $M(t)$, and $c(x)$ agree with this solution. Thus we have obtained the full time dependent solution for an *arbitrary* time independent input $I(x)$. In the limit $x \to 0$ and $t \to \infty$, with the scaling variable $z = xt$ kept finite, the third term in the sum of Eq. (4.45) dominates, and the anticipated scaling behavior of (4.40) is recovered with $F(z) = F_3(z)$.

4.4 Geometrical Fragmentation

It is natural to think of fragmentation geometrically, especially when dropping a plate that shatters when it hits the floor. In this section, we discuss a simple fragmentation model that incorporates the effects of fragment shape. This geometrical fragmentation is characterized by an infinite number of unexpected "hidden" conservation laws. A remarkable consequence of these conservation laws is that the fragment size distribution exhibits both conventional scaling and multifractal scaling.

A minimalist way to incorporate shape into a fragmentation process is the following breaking rule: starting with a rectangle of any shape, a random point inside the rectangle is chosen and then a crack—either horizontal or vertical—fragments the rectangle into two smaller rectangles whose areas equal that of the initial rectangle (Fig. 4.5). Since one fragment is destroyed but two are created in each breaking event, the average number of fragments equals $N = 1+t$. Area conservation then implies that the average fragment area is $\langle A\rangle = \langle x_1 x_2\rangle = (1+t)^{-1}$.

The system may be characterized by $P(x_1, x_2)$, the distribution of fragments of length x_1 and width x_2. This evolution of this distribution is described by the master equation

$$\frac{\partial P(x_1,x_2)}{\partial t} = -x_1 x_2 P(x_1,x_2) + x_2 \int_{x_1} dy_1\, P(y_1,x_2) + x_1 \int_{x_2} dy_2\, P(x_1,y_2). \tag{4.47}$$

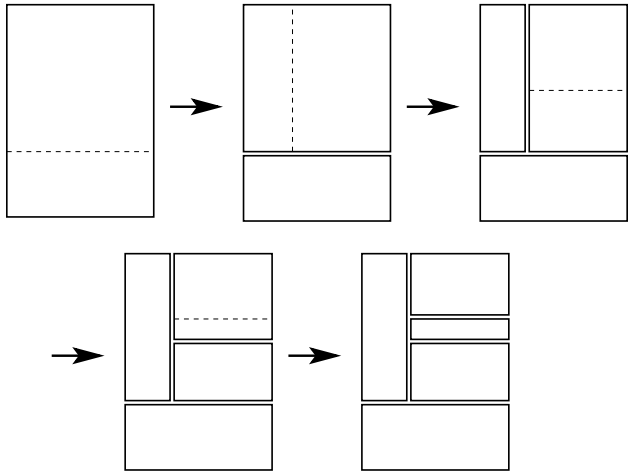

Figure 4.5: First few steps in geometrical fragmentation in two dimensions.

The first term accounts for the loss of a rectangle of area $A = x_1 x_2$ due to its fragmentation. Since the breaking point is chosen randomly inside the rectangle, the overall breaking rate is just proportional to the area. The second term accounts for the gain of a fragment of length x_1 and height x_2 by vertically cracking a fragment of length $y_1 > x_1$ and height x_2. The prefactor x_2 accounts for the fact that the breaking point can be situated anywhere along the vertical crack. The last term accounts for the contribution due to a horizontal crack.

To solve this master equation, we perform the 2-variable Mellin transform. Thus we multiply both sides by $x_1^{s_1-1}x_2^{s_2-1}$ and integrate over all x_1 and x_2. With these steps, the 2-variable Mellin transform $M(s_1, s_2) = \int\int dx_1 dx_2\, x_1^{s_1-1}x_2^{s_2-1}P(x_1, x_2)$ obeys the linear but nonlocal equation

$$\frac{\partial M(s_1, s_2)}{\partial t} = \left(\frac{1}{s_1} + \frac{1}{s_1} - 1\right) M(s_1 + 1, s_2 + 1). \tag{4.48}$$

To put this statement in a more familiar context, note that by the definition of the Mellin transform, the moments of the fragment size are give by

$$\langle x_1^{n_1} x_2^{n_2}\rangle \equiv \frac{M(n_1 + 1, n_2 + 1)}{M(1, 1)}. \tag{4.49}$$

Thus, for example, the total area of all fragments $\mathcal{A}$ is just $M(2, 2)$, while their average area $\langle A\rangle = M(2, 2)/M(1, 1)$. Similarly, the total number of fragments N is just $M(1, 1)$. It is obvious from (4.48) that the total area is conserved and also that the total number of fragments, $N = M(1, 1)$, satisfies $\frac{d}{dt}N = 1$. A much more striking consequence of Eq. (4.48) is the existence of an infinity of conservation laws that are determined by the condition $(s_1^*)^{-1} + (s_2^*)^{-1} = 1$. This family of hidden conservation laws holds in an average sense. That is, while $M(s_1^*, s_2^*)$ does not strictly remain constant after each breaking event, $M(s_1^*, s_2^*)$, averaged over infinitely many realizations of fragmentation is conserved. Only the total area, $M(2, 2)$, is strictly conserved in each breaking event.

Based on the fact that the average fragment size decays algebraically with time in univariate fragmentation with homogeneous breakup kernels, we assume that the leading asymptotic behavior of the Mellin transform is also algebraic in time. Thus we make the ansatz $M(s_1, s_2) \sim t^{-\alpha(s_1,s_2)}$. Substituting this form into (4.48) yields the recursion for the exponent $\alpha(s_1 + 1, s_2 + 1) = \alpha(s_1, s_2) + 1$. The exponent α can now be determined by combining this recursion with the conservation law $\alpha(s_1, s_2) = 0$ anywhere along the curve $(s_1^*)^{-1} + (s_2^*)^{-1} = 1$ to give

$$\alpha(s_1^* + k, s_2^* + k) = k \qquad \text{for all} \qquad (s_1^*)^{-1} + (s_2^*)^{-1} = 1. \tag{4.50}$$

Thus the value of α at an arbitrary point (s_1, s_2) is just the horizontal (or vertical) projection of the distance from this point to the curve $(s_1)^{-1} + (s_2)^{-1} = 1$ along a 45° ray (Fig. 4.6). This distance condition gives

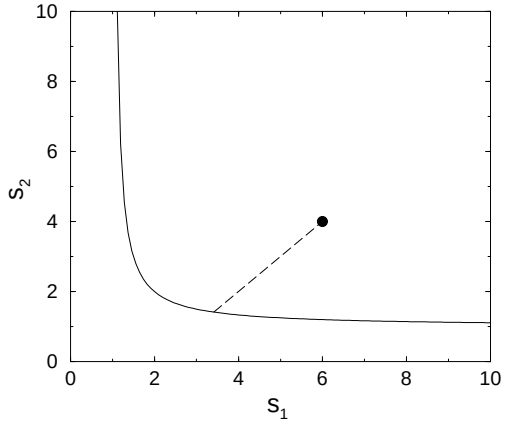

Figure 4.6: Graphical solution of the equation $\alpha(s_1^*+k, s_2^*+k) = k$ with $(s_1^*)^{-1}+(s_2^*)^{-1} = 1$. To solve for the exponent α for a given point (s_1, s_2), a line in the $(1,1)$ direction is drawn from the curve $(s_1^*)^{-1}+(s_2^*)^{-1} = 1$ to (s_1, s_2). The exponent is the length of this line segment.

$(s_1 - \alpha) = s_1^*$ and $(s_2 - \alpha) = s_2^* = [1 - (s_1^*)^{-1}]^{-1}$. Eliminating s_1^* from these two equations, the exponent is the smaller root of the quadratic equation $(s_1 - \alpha)(s_2 - \alpha) - (s_2 - \alpha) = 1$. This gives

$$\alpha(n_1, n_2) = \frac{n_1 + n_2}{2} - 1 - \sqrt{\frac{(n_1 - n_2)^2}{2} + 1},$$

and the leading asymptotic behavior of the moments is given by

$$\langle x_1^{n_1} x_2^{n_2} \rangle \equiv \frac{M(n_1+1, n_2+1)}{M(1,1)} \sim t^{-\alpha(n_1,n_2)-2}, \tag{4.51}$$

This non-linear spectrum of scaling exponents $\alpha(n_1, n_2)$ is an example of *multiscaling*—higher-order moments that are not simply related to low-order moments, *viz.* $\langle x^n \rangle \gg \langle x \rangle^n$. A nice illustration of the consequences of this multiscaling arises in the moments of the fragment length:

$$\langle \ell^n \rangle \equiv \langle x_1^2 \rangle \sim t^{-(n+2-\sqrt{n^2+4})/2}. \tag{4.52}$$

In particular, $\langle \ell \rangle \sim t^{-(3-\sqrt{5})/2} \sim t^{-.382}$ and $\langle \ell^2 \rangle \sim t^{-(2-\sqrt{2})} \sim t^{-.586}$. These moments decay slower than what one might naively anticipate from the behavior of the area. From (4.51), the average area decays as $\langle A \rangle = \langle x_1 x_2 \rangle \sim t^{-1}$, so that the natural length scale obtained from the square-root of the area decays as $t^{-1/2}$. This multiscaling for the length moments stems from the fact that a typical fragment is highly asymmetric (Fig. 4.5). This visual asymmetry can be quantified by the aspect ratio moments $\langle (x_1/x_2)^n \rangle$ which, from Eq. (4.51), diverges as $\langle (x_1/x_2)^n \rangle \sim t^{\sqrt{n^2+1}-1}$.

Although the length and aspect ratio exhibit multiscaling, the area distribution obeys conventional single-parameter scaling in which, again from Eq. (4.51), the area moments are characterized by a linear exponent spectrum: $\langle A^n \rangle \sim t^{-n}$. The area distribution is derived from the multivariate distribution using $P(A,t) = \int\int dx_1 dx_2 P(x_1, x_2)\delta(x_1 x_2 - A)$. The area distribution obeys a scaling form as in Eq. (4.20): $P(x_1, x_2) \simeq t^{-2}\Phi(At)$ with the scaling function

$$\Phi(z) = 6 \int_0^1 d\xi \, (\xi^{-1} - 1) e^{-z/\xi}. \tag{4.53}$$

The area distribution diverges weakly: $\Phi(z) \simeq 6 \ln \frac{1}{z}$ at small areas, $z \ll 1$. In the opposite limit, there is an exponential decay, reminiscent of the one-dimensional case, but with an algebraic correction: $\Phi(z) \simeq 6z^{-2}\exp(-z)$ as $z \gg 1$. The ordinary scaling behavior of the area reflects the fact that the fragmentation rate equals the area.

References

1. E. W. Montroll and R. Simha, J. Chem. Phys. **8**, 721 (1940).
2. A. Charlesby, *Proc. Roy. Soc. London Ser. A* **224**, 120 (1954).
3. T. Harris, *The Theory of Branching Processes* (Berlin: Springer, 1963).
4. R. M. Ziff and E. D. McGrady, J. Phys. A **18**, 3027 (1985).
5. Z. Cheng and S. Redner, Phys. Rev. Lett. **60**, 2450 (1988).
6. S. Redner, in *Statistical Models for the Fracture of Disorder Media*, eds. H. J. Herrmann and S. Roux (North-Holland, 1990).
7. A. F. Filippov, Theory Prob. Appl. **6**, 275 (1991).
8. G. Tarjus and P. Viot, Phys. Rev. Lett. **67**, 1875 (1991).
9. P. L. Krapivsky and E. Ben-Naim, Phys. Rev. E **50**, 3502 (1994).
10. G. J. Rodgers and M. K. Hassan, Phys. Rev. E **50**, 3459 (1994).
11. P. L. Krapivsky, I. Grosse, and E. Ben-Naim, Phys. Rev. E **60**, R993 (2000).
12. E. Ben-Naim and P. L. Krapivsky, Phys. Lett. A **275**, 48 (2000).

Problems

4.1 Exact Solutions

1. Solve the random scission model using the scaling ansatz $P(x,t) \simeq t^2\Phi(xt)$ (see matters of technique).
2. Obtain the leading asymptotic behavior of the moments for the random scission model.

4.4 Geometric Fragmentation

1. Determine the distribution of fragments of length x_1 and height x_2, $P(x_1,x_2)$, for the geometric fragmentation process illustrated below. Show that the two-variable Mellin transform $M(s_1,s_2)$ obeys

$$\frac{\partial M(s_1,s_2)}{\partial t} = \left(\frac{4}{s_1 s_2} - 1\right) M(s_1+1, s_2+1).$$

From this equation and using the assumption that $M(s_1,s_2) \sim t^{-\alpha(s_1,s_2)}$, show that

$$\alpha(n_1,n_2) = \left[(n_1+n_2) - \sqrt{(n_1-n_2)^2+16}\right]/2. \tag{4.54}$$